

Collapse arresting in an inhomogeneous quintic nonlinear Schrödinger model

Yu. B. Gaididei,* J. Schjødt-Eriksen, and P. L. Christiansen

Department of Mathematical Modelling, The Technical University of Denmark, DK-2800 Lyngby, Denmark

(Received 30 November 1998; revised manuscript received 1 June 1999)

Collapse of $(1+1)$ -dimensional beams in the inhomogeneous one-dimensional quintic nonlinear Schrödinger equation is analyzed both numerically and analytically. It is shown that in the vicinity of a narrow *attractive* inhomogeneity, the collapse of beams in which the homogeneous medium would blow up may be delayed and even arrested. [S1063-651X(99)03610-7]

PACS number(s): 42.65.Jx, 03.65.Ge

I. INTRODUCTION

The spatial contraction of wave packets and the formation of a singularity in finite time—the wave collapse or, more generally, the blowup of the wave packet—is one of the basic phenomena in nonlinear physics of wave systems. Examples are the self-focusing of light [1–3] in optics, the collapse of Langmuir waves in plasma [4], the self-focusing of gravity-capillary surface waves [5], the blowup of nonlinear electronic excitations in molecular systems [6], and the collapse in a Bose gas with negative scattering length [7,8]. Wave collapse is an efficient process of energy and/or mass localization as well as energy dissipation (see, e.g., review papers [9–11]).

The theory of self-focusing wave packets in optics, plasma, and solid-state physics is based on the analysis of the nonlinear Schrödinger equation (in the theory of the Bose-Einstein condensation this equation is called the Gross-Pitaevskii equation [12])

$$i \partial_z \psi + \nabla^2 \psi + |\psi|^{2\sigma} \psi + V(\vec{r}) \psi = 0, \quad (1)$$

where $\psi(\vec{r}, z)$ is the complex amplitude of the quasimonochromatic wave train (the condensate wave function), $\nabla^2 = \sum_{i=1}^d \partial_{x_i}^2$ is the d -dimensional Laplace operator, z is the propagation variable (the time variable in Bose-Einstein theory) and $\vec{r} = (x_1, \dots, x_d)$ is the spatial coordinate. The third term in Eq. (1) characterizes the nonlinear properties of the system: light intensity-dependent refractive index in optics, effective self-interaction of Langmuir waves in plasma, or the interaction between Bose particles, etc. Finally the fourth term in Eq. (1) is either an inherent space-dependent refractive index of the material or an external (confining) potential. Physical systems, which share the same value of the factor σd , possess many similar features such as stability properties of the stationary solutions. It was found [10,13] that in homogeneous systems [$V(\vec{r}) = 0$] the stationary solutions of Eq. (1) are stable when $\sigma d < 2$ and unstable when $\sigma d > 2$ with the case $\sigma d = 2$ being marginal. In the latter case the excitation either blows up or disperses depending on whether a certain characteristic measure of the excitation is

above or below a threshold value, respectively. This measure is, e.g., the beam power in optics, the number of atoms in Bose-Einstein condensates, and the number of excitations in plasma physics.

The dynamics of self-focusing waves in inhomogeneous nonlinear systems has become a topic of extensive studies due to the rich dynamical properties induced by the interplay between nonlinearity, dispersion, and inhomogeneity. The effects of periodic spatial modulation of the refractive index [$V(\vec{r}) = v \cos(kx)$] in the spatiotemporal evolution of pulses in nonlinear waveguides were recently investigated using a variational approach and numerical simulations [14], while exact sufficient criteria for blowup were obtained in [15,16].

Feit and Fleck [17] have first pointed out that if nonparaxiality of the beam propagation is taken into account, blowup does not occur. This result was further supported by using a collective coordinate approach [18], by adding an additional term that models the variation of the propagation constant along the direction of propagation [19] and by applying an asymptotic analysis [20,21].

The effect of disorder on the spatiotemporal evolution of pulses in nonlinear waveguides were studied in Ref. [22] where it was shown that random fluctuations delay collapse.

Also, criteria for existence and stability of stationary solutions in inhomogeneous systems have attracted a lot of attention. In [29] modes of an inhomogeneous structure were first found, while a general criterion for the existence of stable stationary solutions was derived in [23].

In physical systems, where an excitation is located in the vicinity of a smooth bell-shaped inhomogeneity with a width much larger than the width of the excitation, one may model the inhomogeneity as a parabolic potential. The possibility of controlling the self-focusing of nonlinear excitations in molecular structures with parabolic-type inhomogeneities was investigated in Ref. [6]. The acceleration of the collapse of light beams in weakly nonlinear dispersive media with either a constant or weakly oscillating parabolic density profile was investigated in Ref. [24]. Collapse and Bose-Einstein condensation in trapped Bose gas with negative scattering length in the presence of the parabolic confining potential, $V(\vec{r}) \sim r^2$, were studied in Refs. [7,8]. However, the parabolic model breaks down when the widths of the inhomogeneity and the excitation are of comparable size. It is the idea of this paper to investigate the dynamical evolution of excitations in the presence of such narrow inhomogeneities.

*Permanent address: Bogolyubov Institute for Theoretical Physics, 252 143 Kiev, Ukraine.

To meet this end we use the one-dimensional quintic nonlinear Schrödinger equation (NLSE) as our model. A key element in this investigation is to show how the collapse of excitations, which are characterized as supercritical in the homogeneous case, may be delayed or even arrested when a narrow attractive inhomogeneity is introduced into the system. As the present model due to the relation $\sigma d=2$, has a close relation to the optical application of the two-dimensional (2D) cubic NLSE [10,13] we will in the following refer to the excitations as beams.

The paper is organized as follows. In Sec. II we introduce the model and describe its basic properties in the homogeneous case before discussing the numerical results obtained when an inhomogeneity is included in the model. From the outcome of the numerical calculations it will become clear that the presence of a narrow attractive inhomogeneity has the potential of postponing or even arresting the formation of a singularity for beams which would collapse in the homogeneous case. In Sec. III we address the problem analytically. Using a certain coordinate transformation enables us to calculate energy radiation from the beam using methods developed to characterize the tunneling of probability in linear quantum-mechanical systems. Finally, Sec. IV summarizes our results.

II. MODEL AND EQUATIONS OF MOTION

To model the propagation of a $(1+1)$ -dimensional beam, $\psi(x,z)$, we use the equation

$$i\psi_z + \psi_{xx} + |\psi|^4\psi + V(x)\psi = 0, \quad (2)$$

where x is a transverse coordinate and z measures the propagation length. In the homogeneous case [$V(x)=0$], Eq. (2) has the stationary solution

$$\psi(x,z) = \Psi(x,\Lambda) e^{i\Lambda z}, \quad (3)$$

where the real shape function $\Psi(x,\Lambda)$ satisfies the equation

$$\frac{d^2\Psi(x,\Lambda)}{dx^2} + \Psi^5(x,\Lambda) - \Psi(x,\Lambda) = 0, \quad (4)$$

which has the solution

$$\Psi(x,\Lambda) = (3\Lambda)^{1/4} \operatorname{sech}^{1/2}(2\sqrt{\Lambda}x) \quad (5)$$

with the mass given by

$$N(\Lambda) \equiv \int_{-\infty}^{\infty} |\psi(x,z)|^2 dx = \frac{\sqrt{3}\pi}{2}. \quad (6)$$

According to the Vakhitov-Kolokolov criterion, the solutions, Eq. (3), are stable and unstable if $dN/d\Lambda > 0$ and $dN/d\Lambda < 0$, respectively. As $N(\Lambda)$ from Eq. (6) is seen not to depend on Λ , application of the stability criterion implies marginal stability of the stationary solutions. Thus, if a stationary solution is perturbed in such a way that $N > N_c = \sqrt{3}\pi/2$, a singularity in the intensity profile $|\psi|^2$ appears within finite propagation length. In this case the beam is said to have undergone a collapse. On the other hand, a perturbed stationary solution with $N < N_c$ cannot remain localized and

the beam ultimately disperses completely. This kind of instability also characterizes stationary solutions of the homogeneous 2D NLSE.

The presence of an inhomogeneity may significantly influence the dynamics of beams with arbitrary initial conditions (see, e.g., [25]). In particular, it is our goal to investigate whether the collapse of beams with $N > N_c$ can be postponed or even arrested. To undertake this investigation we will mainly focus on the situation, where the linear part of the operator in Eq. (1), $-\partial_x^2 - V(x)$, supports a bound state. In this case stable stationary solutions with $N < N_c$ exist [23] and it is thus relevant to ask if these bound states act as attractors for certain classes of initial conditions.

When performing the numerical experiments we use a smoothed version of the rectangular potential well,

$$V(x) = \epsilon[\theta(x+a) - \theta(x-a)], \quad (7)$$

where $\theta(x)$ is the Heaviside step function and ϵ and $2a$ are the height and width of the potential, respectively. As initial conditions we use a slightly supercritical ($N > N_c$) perturbation of the amplitude function $\Psi(x,\Lambda)$ given by

$$\psi(x,0) = \Psi(0.99(x-X_0),1), \quad (8)$$

where X_0 determines the initial distance between the centers of the beam and potential. In the first series (Figs. 1–6) of experiments the potential height and width are fixed at $\epsilon = 0.7$ and $a = 1$, while X_0 is varied in order to control the initial strength of beam/potential interaction. As is seen, the beam collapses in two different cases. When the center of the beam initially is localized sufficiently close to $x=0$ the effect of the potential is to enhance the speed of collapse compared to the scenario with $V(x)=0$. This kind of dynamics is illustrated in Fig. 1. On the other hand, a large distance between the beam center and $x=0$ results in negligible coupling between beam and potential. Consequently, the beam collapses in approximately the same way as in the homogeneous system corresponding to Eq. (2). In Fig. 6, $X_0=5$ corresponds to this scenario, while Fig. 5 ($X_0=3.46885$) illustrates how the presence of the potential can increase the propagation length needed for a singularity to develop in the intensity profile. In between the two extremes where collapse occurs, there exists a range of values for the initial position of the beam center, which leads to arrest of the collapse. (See, Figs. 2–4.) One remarkable feature of this process is that the beam radiation is significantly enhanced by the inhomogeneity [26] and as is seen the radiation develops mainly at the side of the beam that is opposite the well. To interpret the outcome of the numerical experiments in a quantitative way it is useful to have measures for the width and center of the beam in the case when the beam in the large propagates as a single localized entity. To meet this end we introduce the quantities

$$R = \int_{-\infty}^{\infty} |\psi|^6 dx, \quad (9)$$

and

$$X = \frac{1}{N} \int_{-\infty}^{\infty} x|\psi|^2 dx, \quad (10)$$

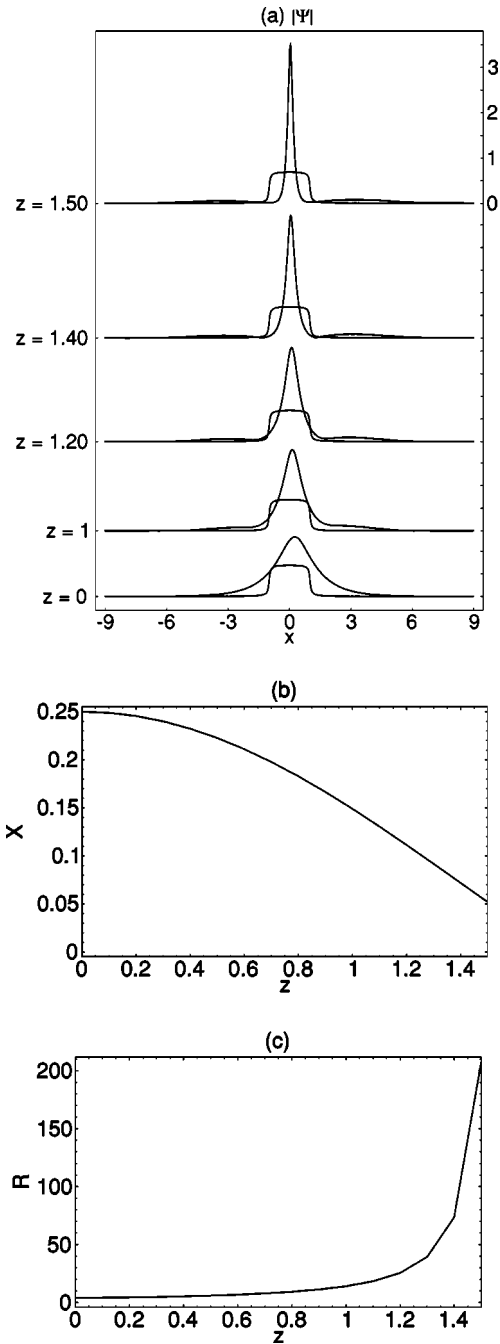


FIG. 1. The half width a of the potential and the height ϵ of the potential are given by 1.0 and 0.7, respectively. The following initial condition for Ψ is used: $\Psi(x,0) = \sqrt{\sqrt{3}} \text{sech}[1.98(x-X_0)]$, where the initial value of the centroid X_0 equals 0.25. In (a) the amplitude of $\Psi(x,z)$, $|\Psi(x,z)|$ is shown for different values of z . In (b) and (c) the centroid, X , and the inverse width squared, $\int |\Psi|^6 dx$, respectively, are plotted versus z .

which in the self-similar approach coincides with the inverse width squared and the position of the maximum intensity, respectively. For a collapsing beam, R diverges and can, therefore, be applied to the outcome of the numerical calculations as a measure of self-focusing. In the experiment shown in Fig. 2(a) where $X_0 = 0.5$, the width decreases until a certain propagation length after which the beam is separated into radiation and a core part. The overall motion of this core part is given by the centroid oscillations in Figs. 2(b) and 2(c),

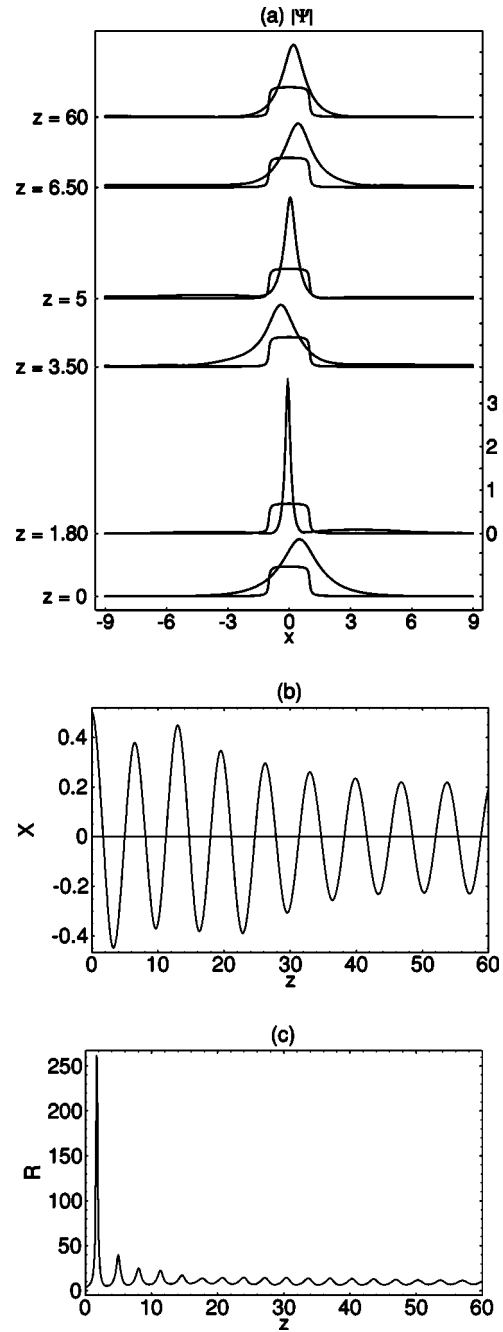


FIG. 2. Same as Fig. 1 with $\epsilon = 0.7$, $a = 1$, and $X_0 = 0.5$.

which initially are accompanied by radiation. However, the emission of radiation decreases as a function of propagation length and is at $z = 60$ no longer visible in Fig. 2(a). In Fig. 3(a), where $X_0 = 2$, the beam is seen to become very quickly distorted by the potential, thus making the interpretation of X and R , as beam center and inverse width squared, valid only initially. Having seen the outcome of the numerical calculations, it is useful to compare the X_0 dependence of the initial centroid acceleration, $X_{zz}(0)$, and the collapse properties of the beam. The centroid acceleration vanishes at $X_0 = 0$ and $X_0 \rightarrow \infty$, while $X_{zz}(0)$ in between these two limits is positive. On the other hand, the beam has been observed to collapse when X_0 is either sufficiently small or large. From this observation we expect the centroid acceleration to facilitate radiation thus enabling the beam mass to drop below N_C ,

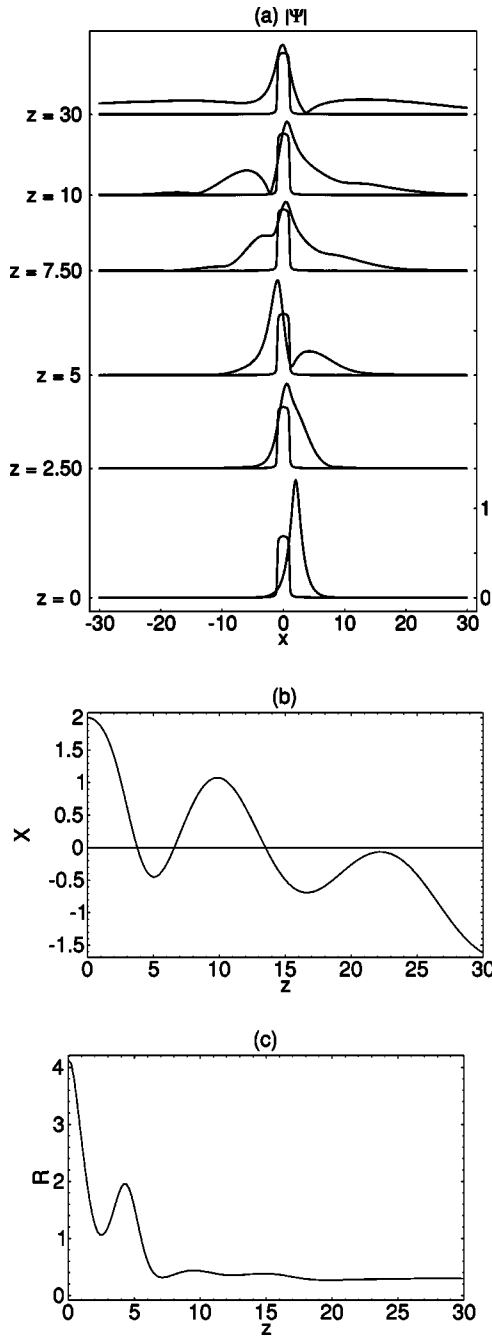


FIG. 3. Same as Fig. 1 with $\epsilon=0.7$, $a=1$, and $X_0=2.0$.

where collapse no longer is possible. This point is subject to rigorous mathematical treatment in the next section.

Another series of experiments, which we performed, was to launch a beam into a system with a negative potential barrier ($\epsilon < 0$). The results of these experiments are shown in Figs. 7(a), 7(b), and 7(c) and Figs. 8(a), 8(b) and 8(c). Here the beam either collapses or disperses depending on its initial position with respect to the barrier. A stabilizing effect of the potential has not been observed in this case.

These numerical experiments demonstrate three remarkable features of the dynamics of supercritical beams in inhomogeneous systems: (i) The collapse of the beam can be delayed and even arrested if the initial distance between the centers of the beam and potential well is in a certain interval. The beam collapses when it is either too close or too far

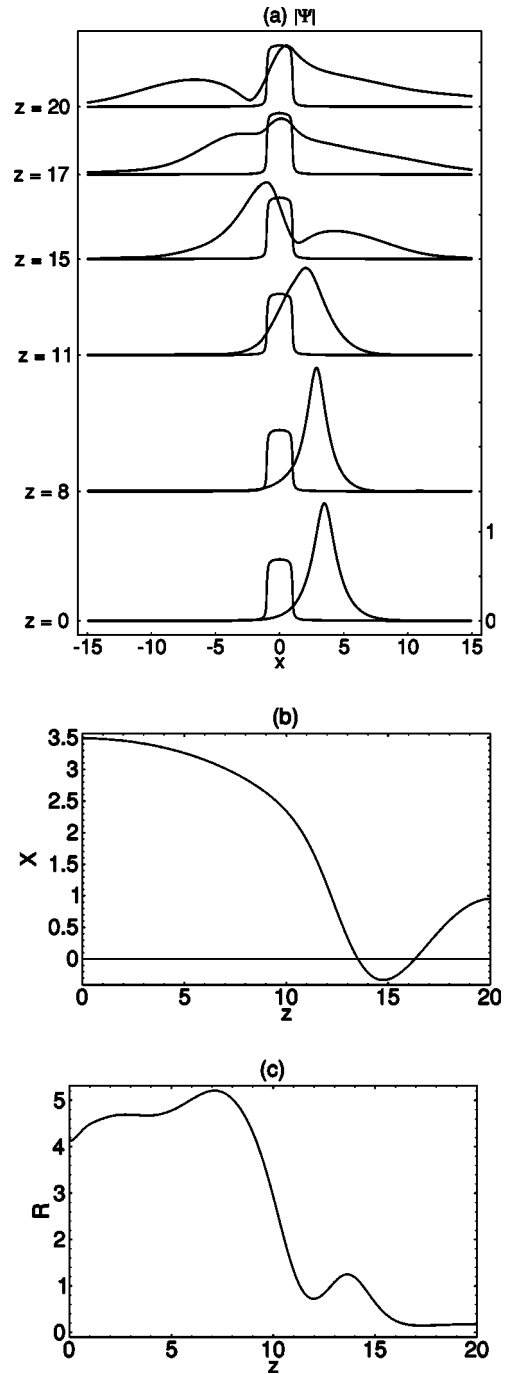


FIG. 4. Same as Fig. 1 with $\epsilon=0.7$, $a=1$, and $X_0=3.46875$.

away from the well. (ii) The inhomogeneity facilitates the radiation of the beam. The radiation occurs mainly in the direction away from the well. (iii) There is a correlation between the centroid motion and the width of the beam.

III. ANALYTICAL RESULTS

In order to give some analytical insight into this problem we introduce the transformation of the noninertial frame of reference in which the centroid of the beam

$$X(z) = \frac{1}{N} \int_{-\infty}^{\infty} x |\psi(x, z)|^2 dx \quad (11)$$

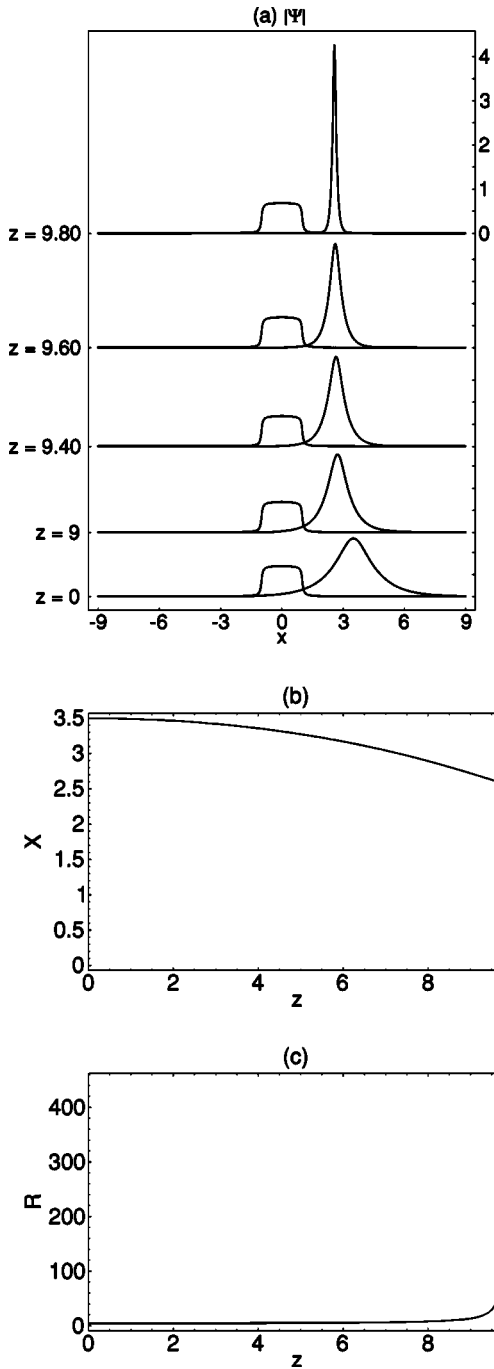


FIG. 5. Same as Fig. 1 with $\epsilon=0.7$, $a=1$, and $X_0=3.46885$.

is at rest. Thus,

$$\psi(x,z) = \bar{\psi}(\bar{x},z) \exp\left(ik(z)\bar{x} + i \int_0^z k^2(z') dz'\right), \quad (12)$$

where $\bar{x} = x - X(z)$ is the transversal coordinate in the new frame of reference and $k(z) = \frac{1}{2}\dot{X}$ is the momentum canonically conjugated to the centroid coordinate (dot denotes the derivative d/dz). In the new frame of reference, Eq. (2) takes the form

$$i \bar{\psi}_z + \bar{\psi}_{\bar{x}\bar{x}} + |\bar{\psi}|^4 \bar{\psi} + V(\bar{x} + X(z)) \bar{\psi} - \frac{1}{2} \ddot{X} \bar{x} \bar{\psi} = 0. \quad (13)$$

The centroid coordinate $X(z)$ satisfies the equation

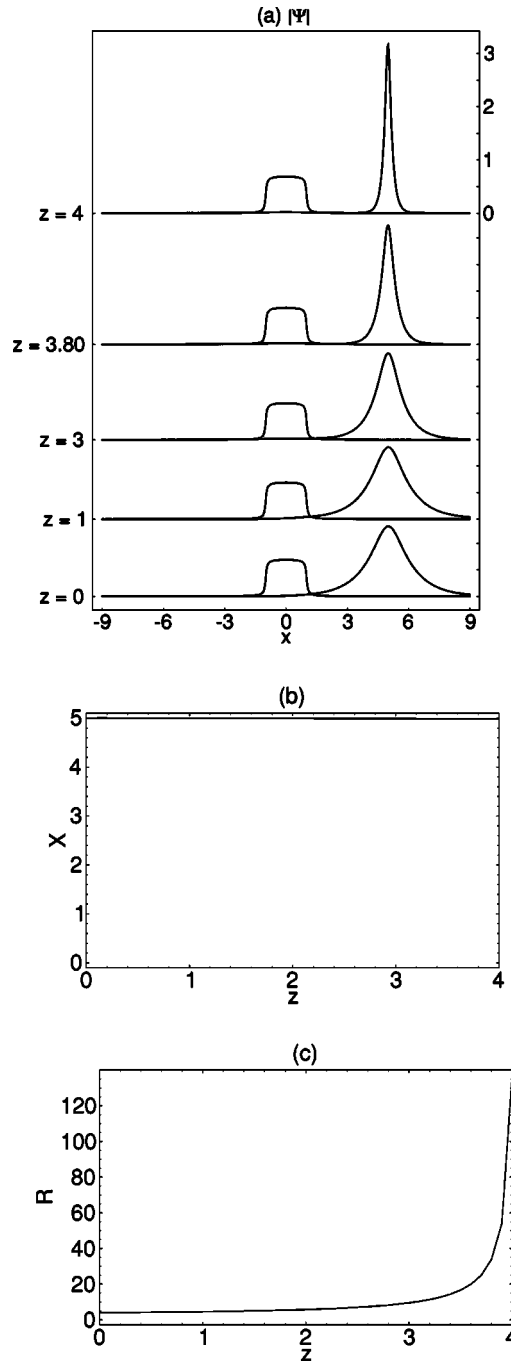


FIG. 6. Same as Fig. 1 with $\epsilon=0.7$, $a=1$, and $X_0=5.0$.

$$\frac{1}{2} \ddot{X} = \frac{1}{N} \int_{-\infty}^{\infty} |\psi(x,z)|^2 \frac{dV(x)}{dx} dx. \quad (14)$$

The fourth term on the right hand side of Eq. (13) describes the influence of the linear potential in the new frame of reference while the fifth term represents the inertial force work. It is worth noticing that due to Eqs. (13) and (14) the function $\bar{\psi}(x,z)$ should satisfy the following compatibility condition:

$$\int_{-\infty}^{\infty} x |\bar{\psi}(x,z)|^2 dx = 0. \quad (15)$$

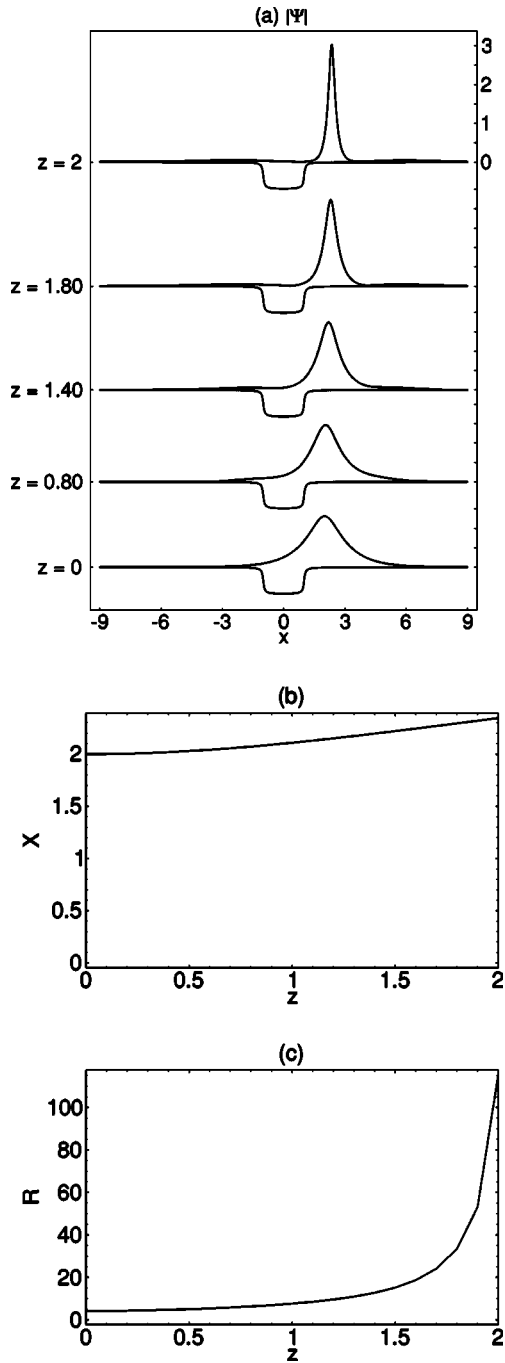


FIG. 7. Same as Fig. 1 with $\epsilon = -0.7$, $a = 1$, and $X_0 = 2.0$.

Using the lens transformation first used in the homogeneous case in [27]

$$\bar{\psi}(\bar{x}, z) = \frac{1}{\sqrt{L(z)}} \Phi(\xi, \zeta) \exp\left(i\zeta + i \frac{L}{L(z)} \frac{x^2}{4}\right), \quad (16)$$

where $L(z)$ is the beam width, and new independent variables are defined as

$$\xi = \frac{\bar{x}}{L(z)}, \quad \zeta = \frac{1}{L^2(z)}, \quad (17)$$

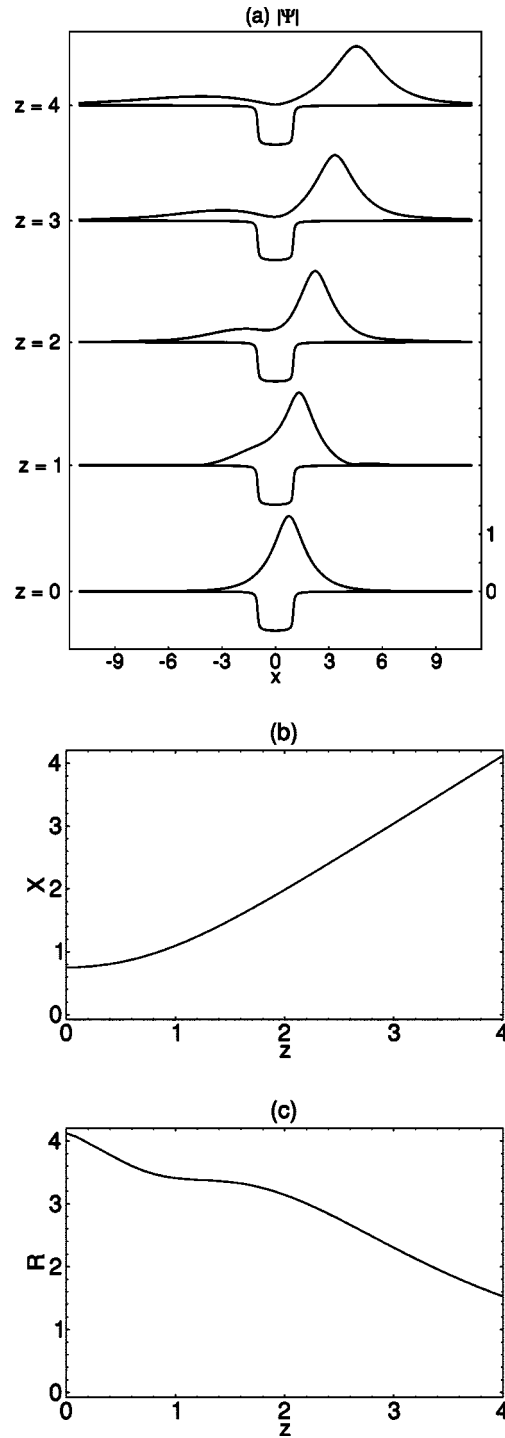


FIG. 8. Same as Fig. 1 with $\epsilon = -0.7$, $a = 1$, and $X_0 = 0.75$.

we obtain from Eq. (13) the equation for the shape function $\Phi(\xi, \zeta)$ in the form

$$i \Phi_\zeta + \Phi_{\xi\xi} + |\Phi|^4 \Phi - \Phi - L^2 W(\xi) \Phi = 0, \quad (18)$$

where

$$W(\xi) = -\frac{1}{4} \xi^2 \beta(z) / L^2 + \epsilon F(\xi, L, X) \quad (19)$$

and

$$\epsilon F(\xi, L, X) = \frac{1}{2} \ddot{X} L \xi - V(\xi L + X) \quad (20)$$

with

$$\ddot{L}L^3 = -\beta(z). \quad (21)$$

The potential $W(\xi)$ represents the influence of inertial forces (the centrifugal potential $-\frac{1}{4}\beta(z)/L^2\xi^2$ and the potential $\frac{1}{2}\ddot{X}L\xi$ of accelerated centroid motion) and of the potential $[-V(\xi L+X)]$, not found in the homogeneous case, on the beam dynamics. When $L(z)$ is known Eqs. (14), (18), and (19) describe the beam evolution.

In the homogeneous case [$V(x)=0$] when Eq. (2) describes a critical collapse, the function $\beta(z)$ that in this case is related to the excess mass above the critical mass N_c through

$$\beta = \frac{N - N_c}{M}, \quad M = \frac{1}{4} \int_{-\infty}^{\infty} x^2 \Psi^2(x, 1) dx = \frac{\sqrt{3} \pi^3}{128}. \quad (22)$$

From Refs. [28–35] is known that $\beta(z)$ satisfies the equation

$$\dot{\beta} = -\frac{8\sqrt{3}}{M L^2} \exp\left(-\frac{\pi}{\sqrt{\beta}}\right). \quad (23)$$

This equation can be obtained from the solvability condition for the asymptotic expansion of the self-similar shape function $\Phi(\xi, \zeta)$ [28–33] or by using a multiscales approach [35].

Let us consider now the beam evolution in the presence of the linear potential $V(x)$. It is assumed that (i) inhomogeneity is weak: the linear part of the potential $V(x)$ is of small intensity ($\max\{|V(x)|\} = \epsilon < 1$) and narrow [$V(x) \approx 0$ when $|x| \leq a$]. We are interested in the case of narrow inhomogeneity because if the inhomogeneity is very broad compared to the width of the beam, the shape of the inhomogeneity can be Taylor expanded around the center of the beam yielding a parabolic potential in the NLSE. This case was investigated in Refs. [6,24]. However, if the width of the inhomogeneity is of the same order as the beam width, the Taylor expansion is no longer valid and one should then, as we did, use a potential that is nonparabolic. (ii) Supercriticality is small: the mass of the beam only slightly differs from the critical value, i.e., $N - N_c / N_c \ll 1$.

Let us represent the wave function $\bar{\psi}(\bar{x}, z)$ in the noninertial frame of reference as

$$\bar{\psi}(\bar{x}, z) = \begin{cases} \psi_s & \text{if } -\xi_l L(z) \leq \bar{x} \leq \xi_r L(z) \\ \psi_o & \text{if } \bar{x} > \xi_r L(z) \text{ or } \bar{x} < -\xi_l L(z), \end{cases}$$

where ψ_s is the inner core function and ψ_o is its outer part. ξ_r ($\xi_r \gg 1$) and ξ_l ($\xi_l \gg 1$) are constants, which characterize the size of the beam. It is worth noting that in the presence of inhomogeneity the beam may be asymmetric and therefore in principle $\xi_r \neq \xi_l$. The mass of the inner core of the beam (in what follows we will call this part of the beam mass the core mass) is

$$N_s = \int_{-\xi_l L(z)}^{\xi_r L(z)} |\bar{\psi}(x, z)|^2 dx = \int_{-\xi_l}^{\xi_r} |\Phi_s(\xi, \zeta)|^2 d\xi. \quad (24)$$

When $\beta=0$ and $\epsilon=0$, Eq. (18) has the stationary solution [see Eqs. (4) and (5)]

$$\Psi \equiv \Psi(\xi, 1) = 3^{1/4} \operatorname{sech}^{1/2}(2\xi). \quad (25)$$

For small β and ϵ one can expect that the function $\Phi(\xi, \zeta)$ has a very small derivative Φ_ζ and thus Eq. (18) has a quasistationary solution Φ_s close to solution (25) in the range

$$|\xi| \leq \xi_0 \ll \xi_j, \quad (j=r, l),$$

$$\beta \xi_0^2 \ll 1, \quad |\ddot{X} L^3 \xi_0| \ll 1. \quad (26)$$

First we want to calculate the core mass N_s in the presence of inertia forces and inhomogeneity. We are looking for a quasistationary solution of Eqs. (18) and (19) in the form

$$\Phi_s = (\Psi + \beta S + \epsilon T) e^{i\epsilon \lambda \xi}, \quad (27)$$

where λ is the eigenfrequency shift caused by the potential $V(x)$. Substituting expansion (27) into Eqs. (18) and (19), it is found that

$$\mathcal{L}S = -\frac{1}{4}\xi^2\Psi, \quad (28)$$

$$\mathcal{L}T = -F\Psi + \lambda\Psi, \quad (29)$$

where $\mathcal{L} = \partial^2/\partial\xi^2 + 5\Psi^4 - 1$. Equations (28) and (29) are always solvable because the zero-mode function is orthogonal to the right-hand side of Eq. (28) due to the symmetry of the function $\Psi(\xi)$. It is also orthogonal to the right-hand side of Eq. (29) because the orthogonality condition

$$\int_{-\infty}^{\infty} \left[\frac{1}{2}\ddot{X}\xi + \frac{1}{L}V(\xi L+X) \right] \Psi \Psi_\xi d\xi = 0 \quad (30)$$

may be rewritten in the form

$$\frac{1}{2}\ddot{X}N_c - \frac{\partial}{\partial X}\mathcal{V}(L, X) = 0, \quad (31)$$

where

$$\begin{aligned} \mathcal{V}(L, X) &= \int_{-\infty}^{\infty} \Psi^2(\xi) V(\xi L+X) d\xi \\ &\equiv \int_{-\infty}^{\infty} V(x) \Psi^2\left(\frac{x-X}{L}\right) dx \end{aligned} \quad (32)$$

is an effective potential caused by the presence of the linear potential $V(x)$. Comparing Eqs. (14) and solvability condition (31), they are seen to coincide if $|\psi| = (1/\sqrt{L})\Psi(\xi L+X)$ in the equation for centroid motion (14).

Using the relation $\mathcal{L}(\partial\Psi(\xi, \Lambda)/\partial\Lambda)_{\Lambda=1} = \Psi$ where the function $\Psi(\xi, \Lambda)$ is given by Eq. (5), one obtains that

$$\int_{-\infty}^{\infty} \Psi S d\xi = -\frac{1}{4} \int_{-\infty}^{\infty} \xi^2 \Psi \left(\frac{\partial\Psi(\xi, \Lambda)}{\partial\Lambda} \right)_{\Lambda=1} d\xi = \frac{1}{2} M, \quad (33)$$

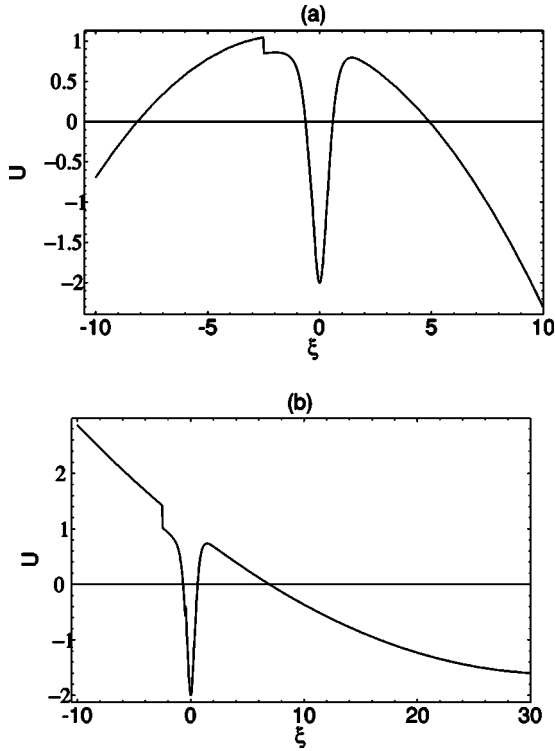


FIG. 9. In (a) and (b) the potential function $U(\xi)$ is depicted for $\beta > 0$ and $\beta < 0$, respectively.

$$\int_{-\infty}^{\infty} \Psi T d\xi = \int_{-\infty}^{\infty} (\lambda \Psi - F \Psi) \left(\frac{\partial \Psi(\xi, \Lambda)}{\partial \Lambda} \right)_{\Lambda=1} d\xi$$

$$= \frac{L^3}{4} \frac{\partial}{\partial L} \mathcal{V}(L, X). \quad (34)$$

Substituting expansion (27) into Eq. (24) and taking into account Eqs. (34) and (32), one obtains the expression for the core mass,

$$N_s = \int_{-\xi_l}^{\xi_r} (\Psi + \beta S + \epsilon T)^2 d\xi \simeq \int_{-\infty}^{\infty} (\Psi^2 + 2\beta \Psi S + 2\epsilon \Psi T)$$

$$= N_c + M\beta + \frac{L^3}{2} \frac{\partial}{\partial L} \mathcal{V}(L, X). \quad (35)$$

This equation gives the link between the core mass N_s , its width L , and centroid X .

We shall obtain an equation for N_s by considering the radiation rate for the core mass. For this purpose it is convenient to rewrite Eqs. (18) and (19) as the Schrödinger equation

$$i\Phi_{\xi} = -\Phi_{\xi\xi} + U(\xi)\Phi,$$

$$U(\xi) = 1 - \frac{1}{4}\beta\xi^2 + \frac{1}{2}\ddot{X}L^3\xi - L^2 V(\xi L + X) - |\Phi|^4. \quad (36)$$

The potential profile $U(\xi)$ for the case when the inhomogeneity potential $V(x)$ is a rectangular potential well [see Eq. (7)] is shown in Fig. 9. The potential energy of inertial forces ($\frac{1}{4}\beta\xi^2$ and $\frac{1}{2}\ddot{X}L^3\xi$) makes the function $U(\xi)$ unbounded from below and as a result the motion of a particle in this potential becomes infinite. This situation is closely related to

the theory of the Stark effect in atoms [36] where even a weak electric field is sufficient to create a potential barrier and makes it possible for electrons to escape from the nucleus.

It is worth noting that the accelerated center of motion potential ($\frac{1}{2}\ddot{X}L^3\xi$) significantly modifies the potential profile $U(\xi)$ making the profile asymmetric and facilitating the escape to the side opposite the position of the inhomogeneity.

From Eq. (18) we obtain that the radiation rate for the core mass is given by

$$\frac{d}{dt} N_s = -J,$$

$$J \equiv J_r + J_l,$$

$$J_r \equiv -\frac{1}{L^2} (i\Phi^* \Phi_{\xi} + \text{c.c.})|_{\xi=\xi_r},$$

$$J_l \equiv \frac{1}{L^2} (i\Phi^* \Phi_{\xi} + \text{c.c.})|_{\xi=-\xi_l}, \quad (37)$$

where J_r (J_l) is the current density (radiation flux) to the right (left) of the beam. The derivation of the expression for the current density J is rather cumbersome and is given in the Appendix. Here we present only the final result. When the centrifugal coefficient β is positive the current densities may be present as follows:

$$J_j = \frac{4}{L^2} \sqrt{3} D_j \quad (j=r, l),$$

$$D_r = \exp \left\{ -\frac{2}{\sqrt{\beta}} \left(\frac{\pi}{2} (1 + \kappa^2) + \kappa + (1 + \kappa^2) \arctan(\kappa) \right) \right\},$$

$$D_l = \exp \left\{ -\frac{2}{\sqrt{\beta}} \left(\frac{\pi}{2} (1 + \kappa^2) - \kappa - (1 + \kappa^2) \arctan(\kappa) \right) \right\}, \quad (38)$$

where the notation

$$\kappa = \frac{\ddot{X}L^3}{2\beta} \quad (39)$$

is used. Here D_r (D_l) is the transmission coefficient for the right (left) potential barrier in the potential profile $U(\xi)$.

In accordance with Eqs. (25) and (32) for the inhomogeneity potential $V(x)$ given by Eq. (7) the effective potential $\mathcal{V}(L, X)$ has the form

$$\mathcal{V}(L, X) = \epsilon \sqrt{3} \left(\arctan \exp \left\{ 2 \frac{a-X}{L} \right\} \right.$$

$$\left. - \arctan \exp \left\{ -2 \frac{a+X}{L} \right\} \right). \quad (40)$$

The motion for the centroid $X(z)$ is governed by the equation

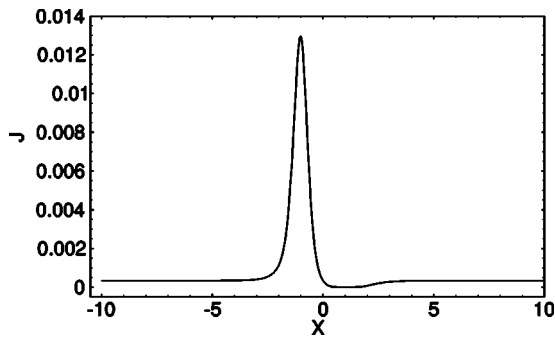


FIG. 10. Plot of the flux to the left for $\beta > 0$. In the figure it is seen that the pulse mainly radiates away from the inhomogeneity.

$$\frac{1}{2} \ddot{X} = \frac{2}{\pi} \frac{\epsilon}{L} \left[\operatorname{sech} \left(2 \frac{X+a}{L} \right) - \operatorname{sech} \left(2 \frac{X-a}{L} \right) \right]. \quad (41)$$

Substituting the centroid acceleration $\frac{1}{2} \ddot{X}$ in form (41) into Eq. (38), one obtains the current density $J_l(X)$ [note that $J_l(X) = J_l(-X)$], which for a given $\beta > 0$ is presented in Fig. 10. As is seen, the current density is a highly asymmet-

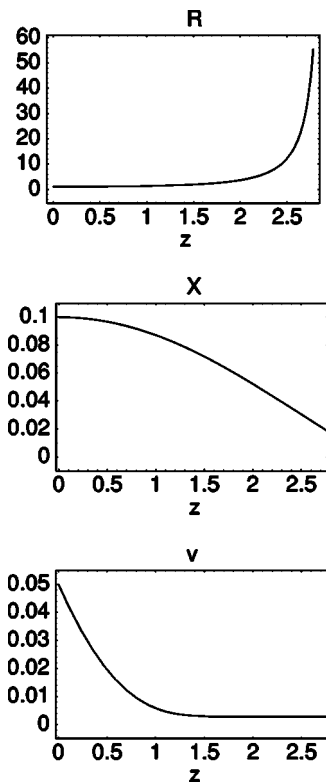


FIG. 11. The half width a of the potential and the height ϵ of the potential are given by 1.0 and 0.2, respectively. The following initial condition for X, \dot{X}, L, \dot{L} , and v are used: $X(0) = 0.1, \dot{X}(0) = 0, L(0) = 1, \dot{L}(0) = 0$, and $v(0) = 0.05$. In the upper figure the inverse width squared, $R = 1/L^2$, is shown as a function of z . In the middle figure the centroid X is depicted versus z . Finally, the lower figure shows the z dependence of v .

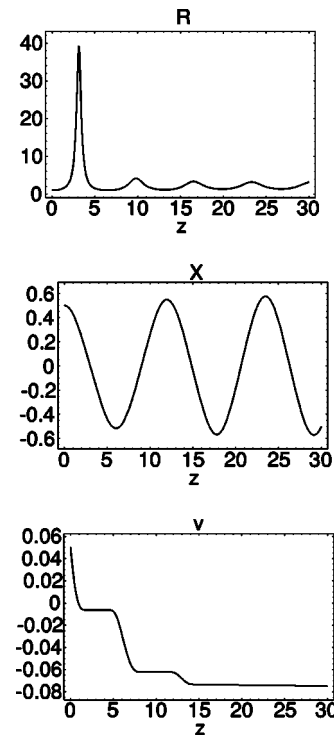


FIG. 12. Same as Fig. 11 with $X(0) = 0.5$.

ric function of X . The beam radiates mainly away from the inhomogeneity. This result is in agreement with the results of numerical simulations shown in Figs. 1(a)–6(a).

When the centrifugal coefficient β is negative the beam

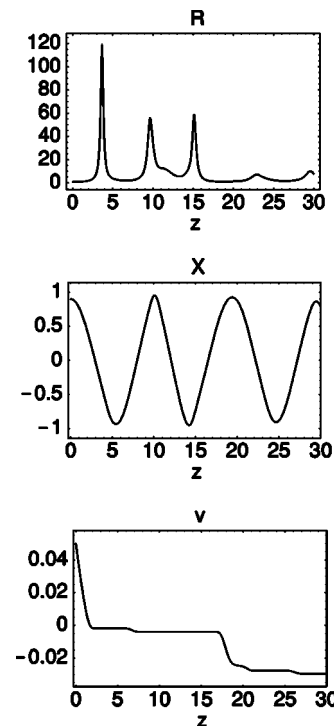


FIG. 13. Same as Fig. 11 with $X(0) = 0.9$.

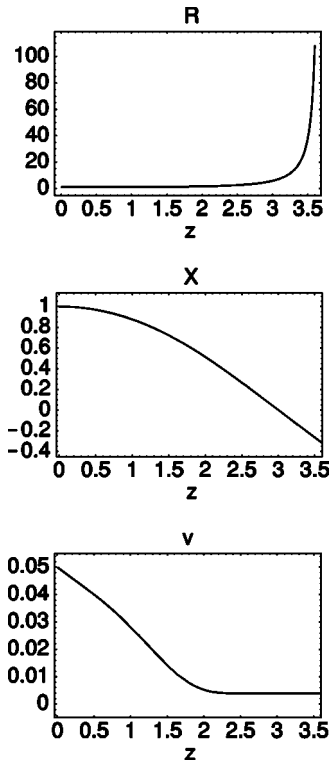


FIG. 14. Same as Fig. 11 with $X(0) = 1.0$.

radiates only to one side, to the side opposite the inhomogeneity [compare the shape of the effective potential $U(\xi)$ in Figs. 9(a) and 9(b)]. The current density in this case has the form

$$J = \frac{4}{L^2} \sqrt{3} D,$$

$$D = \theta(\tilde{X}^2 L^6 + 4\beta) \exp\left\{-2 \sqrt{\frac{1}{|\beta|}} \left[|\kappa| + \frac{1}{2}(1 + \kappa^2) \times \ln\left(\frac{|\kappa| + 1}{|\kappa| - 1}\right)\right]\right\}, \tag{42}$$

where the θ function in front of the exponential function shows that for $\beta < 0$ the radiation may take place only in the presence of relatively strong inhomogeneities.

From Eqs. (37), (38), and (42) we obtain that the radiation rate for the core mass is determined by equation

$$J = \frac{8}{L^2} \sqrt{3} \left(\theta(\beta) \exp\left\{-\pi \frac{1 + \kappa^2}{\sqrt{\beta}}\right\} \times \cosh\left\{2 \frac{1}{\sqrt{\beta}} [\kappa + (1 + \kappa^2) \arctan(\kappa)]\right\} + \theta(-\beta) \theta(\tilde{X}^2 L^6 + 4\beta) \times \exp\left\{-2 \sqrt{\frac{1}{|\beta|}} \left[|\kappa| + \frac{1}{2}(1 + \kappa^2) \ln\left(\frac{|\kappa| + 1}{|\kappa| - 1}\right)\right]\right\} \right). \tag{43}$$

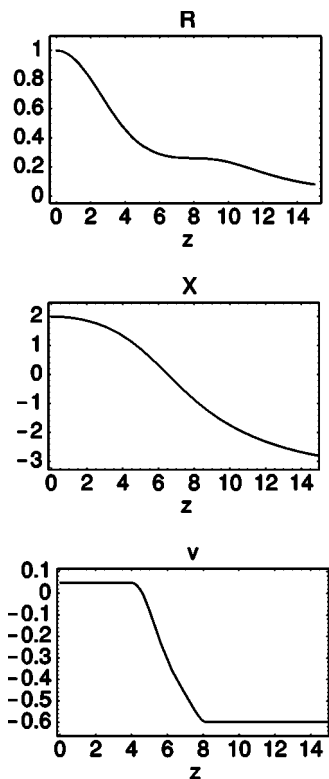


FIG. 15. Same as Fig. 11 with $X(0) = 2.0$.

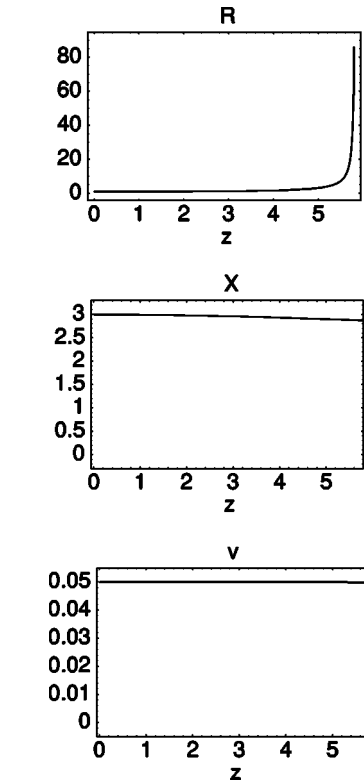


FIG. 16. Same as Fig. 11 with $X(0) = 3.0$.

This expression may be reduced to a more simple form in limiting cases of weak and strong inhomogeneities:

$$J = \frac{8}{L^2} \sqrt{3} \times \begin{cases} \exp\left(-\frac{\pi}{\sqrt{\beta}}\right) & \text{if } \beta/L^3 \gg |\ddot{X}| \\ \exp\left(-\frac{4}{3} \frac{2}{|\ddot{X}L^3}\right) & \text{if } |\beta|/L^3 \ll |\ddot{X}|. \end{cases}$$

Thus in the case of weak inhomogeneity the radiation rate is mainly determined by the centrifugal inertia force $[\beta(z)]$ while in the case of relatively strong inhomogeneity it is due to accelerated centroid motion ($\frac{1}{2}\ddot{X}$).

Combining Eqs. (21), (31), (35), and (37), one obtains that the set of ordinary differential equations, which describe the evolution of the parameters of the beam in the presence of inhomogeneity, has the form

$$\dot{L} = -\frac{\nu}{L^3} + \frac{1}{2M} \frac{\partial}{\partial L} \mathcal{V}(L, X), \quad (44)$$

$$\dot{\nu} = -\frac{1}{M} J(\nu, L, X), \quad (45)$$

$$\frac{1}{2} \ddot{X} = \frac{1}{N_c} \frac{\partial}{\partial X} \mathcal{V}(L, X), \quad (46)$$

where $\nu = N_s - N_c/M$ is the excess core mass above critical, $J(\nu, L, X)$ is current density (43) in which the substitution

$$\kappa = \frac{2M}{N_c} L^3 \left(2M\nu - L^3 \frac{\partial}{\partial L} \mathcal{V}(L, X) \right)^{-1} \frac{\partial}{\partial X} \mathcal{V}(L, X) \quad (47)$$

is used, and $\mathcal{V}(L, X)$ is the effective potential given by Eq. (32). It is worth noticing that in the adiabatic approximation when $\dot{\nu} = 0$, the set of Eqs. (44)–(46) coincides with equations, which were obtained in Ref. [37] using a collective coordinate approach. As is seen from Eq. (45) the magnitude of the excess core mass ν controls the speed of self-focusing, whereas the decrease in ν due to radiation in the nonadiabatic case is governed by Eq. (44). Thus a beam collapse is avoided in the case where a sufficiently high radiation rate brings down the excess core mass ν below zero before a singularity has been formed.

We solve numerically the set of Eqs. (44) for the rectangular well inhomogeneity potential $V(x)$ in the form given by Eq. (7). The parameters used are

$$\nu(0) = 0.05, \quad \epsilon = 0.2,$$

$$\begin{aligned} L(0) &= 1, & \dot{L}(0) &= 0, & \dot{X}(0) &= 0, \\ X(0) &= 0.1, 0.5, 0.9, 1, 2, 3. \end{aligned} \quad (48)$$

The results of the simulations are presented in Figs. 11–16. As is seen for a given degree of super criticality ν and strength of the inhomogeneity ϵ the beam evolution depends

on the initial distance between the beam and the center of the inhomogeneity potential. Collapse arresting and stabilizing of the excitation takes place for $X(0) = 0.75$ and $X(0) = 0.9$, while for $X(0) = 2$ the excitation disperses. These results are in qualitative agreement with numerical studies presented in the previous section.

It is worth noting that tunneling effects here are essential: in the vicinity of inhomogeneity the radiation rate increases and, therefore, the mass of the beam varies with z ($N_s = N_c + M\nu$). The centroid motion and variations of the width of the beam and its mass are obviously correlated.

IV. SUMMARY

In summary we have shown in this paper that the presence of inhomogeneity permits the stabilization of otherwise collapsing excitations. We have shown this via analytical analysis and via numerical simulations. Analyzing the beam dynamics under the influence of attractive inhomogeneity one can conclude that the collapse of the beam can be delayed and even arrested if the initial distance between the beam and the well is in a certain interval. The inhomogeneity facilitates the radiation of the beam. The mass of the beam decreases and becomes less than critical. In this way the singular behavior of the beam is prevented. Analytical and numerical anisotropy of the radiation rate for the beam in the presence of inhomogeneity was observed. The radiation occurs mainly into the direction opposite the well position. We have also shown that there is a correlation between the centroid motion and the width of the beam and its mass.

In view of the similarity between the dynamics of the two-dimensional cubic nonlinear Schrödinger equation and the one-dimensional quintic nonlinear Schrödinger equation [10], our results indicate that two-dimensional supercritical beams propagating in nonlinear waveguides can be controlled by inhomogeneities effects, at least when the supercriticality is not very big (the relative difference between the beam power and the critical power is small). The same scenario could be important in the modeling of Bose-Einstein condensation in trapped atomic gases.

ACKNOWLEDGMENTS

J.B. Keller and Jens Juul Rasmussen are thanked for helpful discussions. Kim Ørskov Ramussen is acknowledged for his contribution to an early stage of this paper. G. Papanicolaou, G. Fibich, and D. Pelinovsky are acknowledged for providing the preprints of their works. Yu.B.G. thanks MIDIT and the Department of Mathematical Modeling, Technical University of Denmark for hospitality. He acknowledges also partial support from the Ukrainian Fundamental Research Fund under Grant No. 2.4/355. The present paper was supported by the Danish Research Council through Contract No. 9313393.

APPENDIX

In this appendix we derive an equation for the radiation rate for the core mass. In this derivation we will use the procedure presented in the review paper [21] (this approach was proposed by Malkin in [38]).

From Eq. (18) we obtain that the radiation rate for the beam mass is given by

$$\begin{aligned} \frac{d}{dz} N_s &= -J, \\ J &= J_r + J_l, \\ J_r &= -\frac{1}{L^2} (i\Phi^* \Phi_\xi + \text{c.c.})|_{\xi=\xi_r}, \\ J_l &= \frac{1}{L^2} (i\Phi^* \Phi_\xi + \text{c.c.})|_{\xi=-\xi_l}, \end{aligned} \quad (\text{A1})$$

where J_r (J_l) is the current density to the right (left) of the beam. As was mentioned above in the case of supercriticality (small β) and weak inhomogeneity, one can neglect the small term $i\Phi_\xi$. Then, Eq. (18) takes the form

$$\begin{aligned} \Phi_{\xi\xi} - U\Phi &= 0, \\ U &= 1 - \frac{1}{4}\beta\xi^2 + \frac{\ddot{X}}{2}L^3\xi - L^2V(\xi L + X) - |\Phi|^4. \end{aligned} \quad (\text{A2})$$

Let us consider separately the cases of β positive and negative. When

$$0 < \beta \sim |\ddot{X}L^3|^2 \ll 1, \quad (\text{A3})$$

the potential U has four turning points (see Fig. 9): two inner (core) turning points

$$\begin{aligned} 0 < \xi_r^c &= \mathcal{O}(1), \\ 0 > \xi_l^c &= \mathcal{O}(1), \end{aligned} \quad (\text{A4})$$

and two outer turning points

$$\begin{aligned} \xi_r^o &= \frac{2}{\sqrt{\beta}}(\kappa + \sqrt{1 + \kappa^2}), \\ \xi_l^o &= \frac{2}{\sqrt{\beta}}(\kappa - \sqrt{1 + \kappa^2}), \end{aligned} \quad (\text{A5})$$

where the notation $\kappa = \ddot{X}L^3/2\sqrt{\beta}$ is used. It is worth noting that the potential $V(\xi L + X)$ does not contribute essentially to the position of the outer turning points due to its narrow character. As it follows from Eq. (A3) an inequality, $|\xi_j^o| \gg 1$ ($j = r, l$), takes place.

To calculate current densities (A1) we will set ξ_r (ξ_l) to be just past the outer turning point ξ_r^o (ξ_l^o) to the right (to the left). It can be done because in the classically inaccessible regions $\xi_r^c < \xi < \xi_r^o$ ($\xi_l^c < \xi < \xi_l^o$), the function $\Phi(\xi)$ decreases exponentially and such a shift will result in an exponentially small contribution to the core mass N_s .

Let us consider first the current density to the right of the beam J_r . When

$$1 \ll \xi \ll \xi_r^o, \quad (\text{A6})$$

we obtain from Eq. (A1)

$$\Phi(\xi) \approx 3^{1/4} e^{-\xi}. \quad (\text{A7})$$

When $\xi > \xi_r^o$ we can neglect the nonlinear term and the potential V in Eq. (A1) and in the WKB approximation (see, e.g., [36]) get

$$\Phi(\xi) \approx \frac{C_r}{\sqrt{p(\xi)}} \exp\left(i \int_{\xi_r^o}^{\xi} p(\bar{\xi}) d\bar{\xi} - i \frac{\pi}{4}\right), \quad (\text{A8})$$

where

$$p(\xi) = \sqrt{U} = \frac{\sqrt{\beta}}{2} \sqrt{(\xi - \xi_r^o)(\xi - \xi_l^o)} \quad (\text{A9})$$

is the quasiclassical momentum and C_r is a constant.

Using the connection formula of the WKB approach [36], we obtain from Eq. (A9) that for $\xi < \xi_r^o$ the function $\Phi(\xi)$ can be represented in the form

$$\Phi(\xi) \approx -i \frac{C_r}{\sqrt{|p(\xi)|}} \exp\left(i \int_{\xi_r^o}^{\xi} p(\bar{\xi}) d\bar{\xi}\right). \quad (\text{A10})$$

In the interval $1 \ll \xi \ll \xi_r^o$,

$$\left| \int_{\xi_r^o}^{\xi} p(\bar{\xi}) d\bar{\xi} \right| = S_r - \int_0^{\xi} p(\bar{\xi}) d\bar{\xi} \approx S_r - \xi, \quad (\text{A11})$$

where

$$S_r = \int_0^{\xi_r^o} |p(\bar{\xi})| d\bar{\xi} = \frac{1 + \kappa^2}{\sqrt{\beta}} \left(\frac{\pi}{2} + \frac{\kappa}{1 + \kappa^2} + \arctan(\kappa) \right). \quad (\text{A12})$$

Comparing Eqs. (A7) and (A12) we see that inner and outer parts of the function $\Phi(\xi)$ can be matched if

$$C_r = i3^{1/4} \sqrt{2} \exp(-S_r). \quad (\text{A13})$$

It is seen from Eq. (A8) that for $\xi \gg \xi_r^o$ the function $\Phi(\xi)$ has the asymptotic form

$$\Phi(\xi) \approx \frac{C_r}{\sqrt{\xi}} \left(\frac{4}{\beta} \right)^{1/4} \exp\left(i \frac{\sqrt{\beta}}{4} \xi^2 - i \frac{\pi}{4}\right). \quad (\text{A14})$$

Therefore, introducing Eqs. (A13) and (A14) into Eq. (A1), we obtain that the current density to the right of the beam is given by

$$J_r = \frac{4}{L^2} \sqrt{3} D_r, \quad (\text{A15})$$

where

$$D_r = \exp(-2S_r) \quad (\text{A16})$$

is the transmission coefficient for the classically inaccessible region $[\xi_r^c, \xi_r^o]$. In the same way one can obtain that the

current density to the left of the beam has the form

$$J_l = \frac{4}{L^2} \sqrt{3} D_l, \quad (A17)$$

$$D_l = \exp(-2S_l),$$

with D_l being the transmission coefficient for the classically inaccessible region $[\xi_l^c, \xi_l^o]$. Here,

$$S_l = \int_{\xi_l^o}^0 p(\bar{\xi}) d\bar{\xi} = \frac{1 + \kappa^2}{\sqrt{\beta}} \left(\frac{\pi}{2} - \frac{\kappa}{1 + \kappa^2} - \arctan(\kappa) \right). \quad (A18)$$

If we substitute Eqs. (A15) and (A17) into Eq. (A1), we get that the radiation rate for the core mass is

$$\frac{dN_s}{dz} = -\frac{8}{L^2} \sqrt{3} \exp\left(-\pi \frac{1 + \kappa^2}{\sqrt{\beta}}\right) \times \cosh\left\{2 \frac{1}{\sqrt{\beta}} [\kappa + (1 + \kappa^2) \arctan(\kappa)]\right\}. \quad (A19)$$

Note that in the case of homogeneous quintic model when $\ddot{X} \equiv 0$ radiation rate (A19) coincides with the rate that was calculated in Ref. [35].

When $\beta < 0$ outer turning points (A5) exist when

$$\ddot{X}^2 L^6 + 4\beta > 0. \quad (A20)$$

But in contrast to the case of positive β now there is only a one-directional tunneling, to the side opposite the position of inhomogeneity (see Fig. 9). Neglecting the back process of mass trapping due to waves that are reflected from the distant turning point and using the same method as was described above, we obtain for

$$-\ddot{X}^2 L^6 < 4\beta < 0 \quad (A21)$$

that current density has the form

$$J = \frac{4}{L^2} \sqrt{3} D,$$

$$D = \exp(-2S),$$

$$S = \int_0^{\xi^o} p(\bar{\xi}) d\bar{\xi} = \sqrt{\frac{1}{|\beta|}} \left[|\kappa| + \frac{1}{2} (1 + \kappa^2) \ln \left(\frac{|\kappa + 1|}{|\kappa - 1|} \right) \right], \quad (A22)$$

where $\xi^o = \min\{|\xi_r^o|, |\xi_l^o|\}$.

Combining Eqs. (A19) and (A22) we obtain that the radiation rate of the core mass is

$$\frac{dN_s}{dz} = -J,$$

$$J = \frac{8}{L^2} \sqrt{3} \left(\theta(\beta) \exp\left\{-\pi \frac{1 + \kappa^2}{\sqrt{\beta}}\right\} \times \cosh\left\{2 \frac{1}{\sqrt{\beta}} [\kappa + (1 + \kappa^2) \arctan(\kappa)]\right\} + \theta(-\beta) \theta(\ddot{X}^2 L^6 + 4\beta) \times \exp\left\{-2 \sqrt{\frac{2}{|\beta|}} \left[|\kappa| + \frac{1}{2} (1 + \kappa^2) \ln \left(\frac{|\kappa + 1|}{|\kappa - 1|} \right) \right] \right\} \right), \quad (A23)$$

where $\theta(x)$ is the Heaviside step function. Expression (A23) may be significantly simplified for limiting cases:

$$J = \frac{8}{L^2} \sqrt{3} \times \begin{cases} \exp\left(-\frac{\pi}{\sqrt{\beta}}\right) & \text{if } 2\beta/L^3 \gg |\ddot{X}| \\ \exp\left(-\frac{4}{3} \frac{2}{|\ddot{X} L^3|}\right) & \text{if } 2|\beta|/L^3 \ll |\ddot{X}|. \end{cases}$$

Thus, the radiation rate is controlled by two inertia forces: by the centrifugal force β/L^3 and by the inertia force caused by the accelerated center-of-mass motion \ddot{X} .

[1] G.A. Askar'yan, Zh. Éksp. Teor. Fiz. **42**, 1568 (1962) [Sov. Phys. JETP **15**, 1088 (1962)].
 [2] R.J. Chiao, F. Gardmire, and C.H. Townes, Phys. Rev. Lett. **13**, 479 (1964).
 [3] P. Kelley, Phys. Rev. Lett. **15**, 1005 (1965).
 [4] V.E. Zakharov, Zh. Éksp. Teor. Fiz. **62**, 1745 (1972) [Sov. Phys. JETP **35**, 908 (1972)].
 [5] G. Papanicolau, C. Sulem, P.L. Sulem, and X.P. Wang, Physica D **72**, 61 (1994).

[6] Yu.B. Gaididei, K.Ø. Rasmussen, and P.L. Christiansen, Phys. Rev. E **52**, 2951 (1995).
 [7] E.V. Shuryak, Phys. Rev. A **54**, 3151 (1996).
 [8] Yu. Kagan, A.E. Muryshev, and G.V. Shlyapnikov, Phys. Rev. Lett. **81**, 933 (1998).
 [9] V.E. Zakharov, in *Handbook of Plasma Physics*, edited by M.M. Rosenbluth and R.Z. Sagdeev (Elsevier, Amsterdam, 1984), p. 81.
 [10] J. Juul Rasmussen and K. Rypdal, Phys. Scr. **33**, 481 (1986);

- K. Rypdal and J. Juul Rasmussen, *ibid.* **33**, 498 (1986).
- [11] E.A. Kuznetsov, *Chaos* **6**, 381 (1996).
- [12] L.P. Pitaevskii, *Zh. Éksp. Teor. Fiz.* **40**, 646 (1961) [*Sov. Phys. JETP* **13**, 451 (1961)]; E.P. Gross, *Nuovo Cimento* **20**, 454 (1961).
- [13] E.A. Kuznetsov, A.M. Rubenchik, and V.E. Zakharov, *Phys. Rep.* **142**, 103 (1986).
- [14] A.B. Aceves and C. De Angelis, *Opt. Lett.* **18**, 110 (1993).
- [15] S.K. Turitsyn, *Opt. Lett.* **18**, 110 (1993).
- [16] Yu.S. Kivshar and S.K. Turitsyn, *Phys. Rev. E* **49**, R2536 (1994).
- [17] M.D. Feit and J.A. Fleck, Jr., *J. Opt. Soc. Am.* **5**, 633 (1988).
- [18] J.T. Manassah and B. Gross, *Opt. Lett.* **17**, 976 (1992).
- [19] N.N. Akhmediev, A. Ankiewicz, and J.M. Solo-Crespo, *Opt. Lett.* **18**, 411 (1993).
- [20] G. Fibich, *Phys. Rev. Lett.* **76**, 4356 (1996).
- [21] G. Fibich and G. Papanicolaou (unpublished).
- [22] Yu.B. Gaididei and P.L. Christiansen, *Opt. Lett.* **23**, 1090 (1998).
- [23] H.A. Rose and M.I. Weinstein, *Physica D* **30**, 207 (1988).
- [24] L. Bergé, *Phys. Plasmas* **4**, 1227 (1997).
- [25] A.B. Aceves, J.V. Moloney, and A.C. Newell, *Phys. Rev. A* **39**, 1809 (1989).
- [26] It is worth noticing that the enhancement of the beam radiation in the presence of inhomogeneity for the case of the cubic NLSE has been observed in the paper by N.N. Akhmediev, V.I. Korneev, and Yu.V. Kuz'menko, *Zh. Éksp. Teor. Fiz.* **88**, 107 (1985) [*Sov. Phys. JETP* **61**, 62 (1985)].
- [27] V.I. Talanov, *Zh. Éksp. Teor. Fiz. Pis'ma Red.* **11**, 447 (1970) [*JETP Lett.* **11**, 303 (1970)].
- [28] G.M. Fraiman, *Zh. Éksp. Teor. Fiz.* **88**, 390 (1985) [*Sov. Phys. JETP* **61**, 228 (1985)].
- [29] N.N. Akhmediev, *Zh. Éksp. Teor. Fiz.* **83**, 545 (1982) [*Sov. Phys. JETP* **56**, 299 (1982)].
- [30] A.I. Smirnov and G.M. Fraiman, *Physica D* **52**, 2 (1991).
- [31] B.J. LeMesurier, G. Papanicolaou, C. Sulem, and P. Sulem, *Physica D* **32**, 210 (1988).
- [32] M. Landman, G. Papanicolaou, C. Sulem, and P. Sulem, *Phys. Rev. A* **38**, 3837 (1988).
- [33] S. Dyachenko, A.C. Newell, A. Pushkarev, and V.E. Zakharov, *Physica D* **57**, 96 (1992).
- [34] G.S. Luther, A.C. Newell, and J.V. Moloney, *Physica D* **74**, 59 (1994).
- [35] D. Pelinovsky, *Physica D* **119**, 301 (1998).
- [36] L.D. Landau and E.M. Lifshitz, *Quantum Mechanics* (Pergamon Press, Oxford, 1965).
- [37] P.L. Christiansen, Yu.B. Gaididei, M. Johansson, K.Ø. Rasmussen, D. Usero, and L. Vázquez, *Phys. Rev. B* **56**, 14 407 (1997).
- [38] V.M. Malkin, *Phys. Lett. A* **151**, 285 (1990).